A Fast and Robust Super Resolution Method for Intima Reconstruction in Medical Ultrasound

Yuguo Dai , Bo Wang and Dong C.Liu
Computer Science College, Sichuan University,
Chengdu, China
E-mail: daiyuguo@gmail.com , womenzai2005@gmail.com , dongcliu@gmail.com

Abstract—**Accurate measurement of intima-media thickness (IMT) in ultrasound images is clinically meaningful but also difficult because of low resolution. This paper proposes an approach to reconstruct a resolution-enhanced intima from a sequence of acquired images using a maximum a-posteriori framework. Anisotropic diffusion is used to reduce speckle with edge enhancement during reconstruction. For real time application in an ultrasound system, a fast and robust approach is employed in the presence of outliers. Finally, an iterative process is used to achieve a single high-resolution image with a better defined intima boundary than the original images. Our approach may be a valuable preprocessing step to image segmentation and IMT measurement.**

Keywords- super resolution; intima reconstruction; ultrasound image; anisotropic diffusion

I. INTRODUCTION

Ultrasound imaging is an important modality used commonly in clinical diagnosis because of its low cost and high safety. Recent evidence suggests a clear link between the degree of carotid artery atherosclerosis and the carotid artery intima-media thickness (IMT) which can be detected by B-mode ultrasound image. The value of IMT for healthy population is about 0.6mm (0.61mm for female and 0.68mm for male). It will thicken with increasing age, but will not be over 1.0mm. An IMT over 1.0mm indicates the aurae of atherosclerosis. Although precise imaging of intima may result in early diagnosis of cardiovascular disease, sub-millimeter changes are difficult to precisely measure.

Axial resolution in ultrasound is limited by the bandwidth of the transducer, and speckle artifacts pervade the image. Hence, the intima in an intravascular ultrasound (IVUS) image is unclear and discontinuous. Researchers have proposed many approaches for reducing speckle in ultrasound images. Super resolution is an effective method to reconstruct a high resolution (HR) image from several appropriately shifted low resolution (LR) images [1,2], which is widely used for medical imaging, astronomical imaging, infrared imaging, and so on. For intima reconstruction, super resolution is proven to be an effective method with speckle reduction by anisotropic diffusion [3].

Most of previously proposed methods have two main drawbacks. Firstly, an iterative process used in the method requires a long computation time cost. Secondly and more importantly, the input sequence must be manually selected from potentially hundreds of frames. Outliers in a sequence of input images may produce large errors in the algorithm. In this paper, we propose a robust super resolution method much less sensitive to outliers. This allows a more automatic reconstruction process where the input is a random sequence from a cine loop.

The super resolution problem is an ill-posed inverse problem. In this paper, we use a maximum a-posteriori (MAP) approach with transformation information, and we use anisotropic diffusion for regularization. During this process, registration is an important step of the whole algorithm. Incorrect estimated translation may severely affect the result. A frequency domain approach to registration [4] is used in this paper. In addition, proposes a robust method for ultrasound images and provide an efficient implementation. Using in-vivo data taken from the carotid artery, we verify our proposed method and compare it to other methods.

II. MATERIALS AND METHODS

A. Super-resolution model

The goal of super-resolution (SR) is to improve the spatial resolution of an image. This type of problem is an inverse problem, wherein the source of information, or high-resolution (HR) image, is estimated from the observed data, or low-resolution (LR) images. Each of the LR images $\{Y_k, k=1,2,\ldots,N\}$ $[M\times M]$ can be modeled by a sequence of geometric warping, blurring, and downsampling operations on the high resolution $L\times L$ image X , followed by additive noise. We can represent Y_k and X as column vectors with length M^2 and L^2 respectively. The model can be formulated as [2]:

$$Y_k = D_k H_k F_k X + V_k \qquad k = 1,2,\ldots,N \tag{1}$$

where D_k is the downsampling matrix of size $[M^2\times L^2]$, H_k is the blurring matrix of size $[L^2\times L^2]$ representing the ultrasound system's point spread function (PSF), F_k is the geometric warp matrix of size $[L^2\times L^2]$, V_k is the additive noise, and N is the number of available input LR images.

A maximum a-posteriori (MAP) estimator of X maximizes the probability density function (PDF) $P(X|Y_k)$ with respect to

$$X = \arg\max\{P(X \mid Y_1, Y_2, \ldots, Y_N)\} \tag{2}$$

Taking the log function and Bayes rule to the conditional probability, the MAP estimate of X can be expressed as

$$X = \arg\max\{\ln P(Y_1, Y_2, \ldots, Y_N \mid X) + \ln P(X)\} \tag{3}$$

The prior knowledge $P(X)$ of the MAP optimization provides essentially a regularization factor and a Markov random field is often adopted.

$$P(X) = \frac{1}{Z}\exp\{-\phi(X)\} = \frac{1}{Z}\exp\{-\varphi\|\nabla X\|^2\} \tag{4}$$

where Z is a constant, $\phi(X)$ is an energy function, and one of the existing scheme used in (4) is applied in our work.

Assuming the V_k is additive Gaussian noise with mean value of zero and variance of σ_k^2. The conditional probability in (3) can be written as:

$$\begin{aligned} P(Y_1, Y_2, \ldots, Y_N \mid X) &= \prod_{k=0}^{N}(Y_k \mid X) \\ &= \prod_{k=1}^{N}\frac{1}{(2\pi\sigma_k^2)^{\frac{M}{2}}}\exp\left\{-\frac{1}{2\sigma_k^2}\|Y_k - D_k H_k F_k X\|^2\right\} \\ &= \frac{1}{(2\pi\sigma^2)^{\frac{M}{2}}}\exp\left\{-\sum_{k=1}^{N}\frac{1}{2\sigma^2}\|Y_k - D_k H_k F_k X\|^2\right\} \end{aligned} \tag{5}$$

The noise is assumed to be identically distributed with variance of σ^2, which is absorbed by the parameter $\lambda=1/2\sigma^2$. Combining Eqns (3), (4) and (5), and dropping out the irrelevant terms, X can be solved by minimizing the following expression:

$$E = \lambda\sum_{k=1}^{N}\|Y_k - D_k H_k F_k X\|^2 + \varphi(\|\nabla X\|^2) \tag{6}$$

Letting $dE/dX=0$, the equation becomes:

$$\lambda\sum_{k=0}^{N}F_k^T H_k^T D_k^T(D_k H_k F_k X - Y_k) - \nabla \bullet \left[\varphi'(\|\nabla X\|^2)\nabla X\right] = 0 \tag{7}$$

The steepest descent (SD) algorithm is an efficient method to reach the solution X by the following iterative process until an iteration convergence criterion is met:

$$X_{i+1} = X_i - \mu\left[\lambda\sum_{k=1}^{N}F_k^T H_k^T D_k^T(D_k H_k F_k X_i - Y_k) - \nabla \bullet [C\nabla X]\right] \tag{8}$$

and

$$C = \varphi'(\|\nabla X\|^2) = 1/\left[1 + \left(\frac{\|\nabla X\|}{K}\right)^2\right] \tag{9}$$

where μ is the step size, which should be small enough. The second term is the detail recovery term that combines information from different frames to update X, and the last term is a smoothing term, or regularization factor, that suppresses instability. The second term can be implemented by convolution with some appropriate kernels. In this paper, a faster and robust implementation is applied [5]-[8].

B. The fast and robust implement

Because the algorithm is applied in carotid intima reconstruction, the following assumptions are feasible:

- All the input images are the same size, and all the decimation operations are also the same, i.e., $\forall k$, $D_k=D$.
- The sequence input images are acquired by the same ultrasound system at the same depth so all the blur operations are assumed equal, i.e., $\forall k$, $H_k=H$. Moreover, the region-of-interest (ROI) is sufficiently small so that H is assumed to be linear space invariant (LSI), and the matrix H is block circulant.
- The ROI needed to reconstruct the result is small enough so that translational displacement at all points inside may be considered equal. A rigid registration will be applied for motion estimation [5]. Therefore, the matrices F_k are all block circulant and linear space invariant.

With these assumptions, H and F_k are block circulant matrices which commute ($F_kH=HF_k$ and $F_k^T H_k^T = H_k^T F_k^T$).So, the second term in (8) can be written as[7]:

$$\begin{aligned} &\sum_{k=1}^{N}F_k^T H_k^T D_k^T(D_k H_k F_k X_i - Y_k) \\ &= H^T(\sum_{k=1}^{N}F_k^T D^T D F_k^T)HX_i - H^T(\sum_{k=1}^{N}F_k^T D^T Y_k) \\ &= H^T R_0 H X_i - H^T P_0 \end{aligned} \tag{10}$$

where $R_0 = \sum_{k=1}^{N}F_k^T D^T D F_k^T$ and $P_0 = (\sum_{k=1}^{N}F_k^T D^T Y_k)$ (11)

The iterative process is time consuming, and we do not wish to calculate each input image at every iteration. From (10), we see matrices R_0 and P_0 need to be calculated once only for the whole algorithm. The part of the second term can save 80% in run-time compared to the original SD algorithm [7].

To compensate for potential outlier images in the sequence, we propose replacing the summation in (10) with a scaled pixel-wise median to increase robustness [8]. Equations (8) and (11) then become:

$$X_{i+1} = X_i - \mu[\lambda(H^T R_0 H X_i - H^T P_0) - \nabla \bullet (C\nabla X_i)]$$

where

$$\begin{aligned} R_0 &= N \cdot median\{F_k^T D^T D F_k^T\}_{k=1}^{N} \\ P_0 &= N \cdot median\{F_k^T D^T Y_k\}_{k=1}^{N} \end{aligned} \tag{12}$$

Using (12), manually pre-selecting proper frames from a cine loop is no longer necessary.

C. *Edge-Enhancing Super-Resolution*

The improvement in (12) gives a fast and robust method to implement the updates of X corresponding to the second term in (8), but the results will be degraded by speckle noise. In ultrasound imaging, anisotropic diffusion is an effective method to suppress speckle without smoothing edges and may be incorporated into the SR algorithm through the regularization. Perona and Malik's anisotropic diffusion [9] with equation (9) is adopted in this paper and can achieve an edge-enhancing regularization during the super-resolution process.

The iterations of the regularization factor in (12) correspond to the iterations required by anisotropic diffusion. Many researchers have discussed the implementations of the diffusion process. We use a 4-nearest-neighbors discretization scheme:

$$\nabla\bullet(D\nabla X)_{i,j} = [C_N\cdot\nabla_N X + C_S\cdot\nabla_S X + C_E\cdot\nabla_E X + C_W\cdot\nabla_W X]_{i,j} \qquad (13)$$

where N, S, E, W are the subscripts for North, South, East, West, and the gradient indicates nearest-neighbor differences. The threshold K in (9) is a constant fixed by hand at some fixed value [9], and a step size μ has to satisfy $0\leq\mu\leq 0.25$ to be stable following Von Neumann's criteria.

III. Experimental Results

A. *Experiments*

A test using a sequence of acquired carotid images from a commercially available ultrasound system is used to validate the effect on intima reconstruction. A cine loop was obtained using a 7.5MHz probe with a Saset Healthcare iMago c21 at a scanning depth of 3.9 cm. The pulse motion, or throbbing of the artery, can give some translational shift needed for the SR algorithm. Importantly, the ROI we selected should be small enough to avoid too much distortion. We need only a rectangular ROI located near the boundaries with visible intima to reconstruct for precise measurement of the IMT.

Therefore, the rigid registration algorithm can be used on the small ROI, and the pulse motion can give the sub-pixel shifts needed for the SR algorithm. However, probe movement or other internal movement in the patient may produce outliers, i.e., "bad" or inappropriate images for use. Generally, a pre-selection is needed to avoid outliers, but our robust version does not need pre-selection and offers a more practical method on a clinical ultrasound system.

In our test, 16 frames of a sequence images are used for the input small size images including 2 outlier frames which might occur by the reasons explained above, see Fig. 1(a) and 1(b). They will be used to perform the following algorithms with the same number of iterations and same initial estimate and the original small size image (200×200) has been zoomed in to a bigger 800×800 image by bicubic interpolation (factor of 4):

- The fast SR algorithm proposed without the robust process, adding an anisotropic diffusion regularization
- The proposed fast and robust SR algorithm without anisotropic diffusion
- The fast and robust SR algorithm proposed in this paper with anisotropic diffusion speckle reduction

The comparable results are seen in Fig.2.

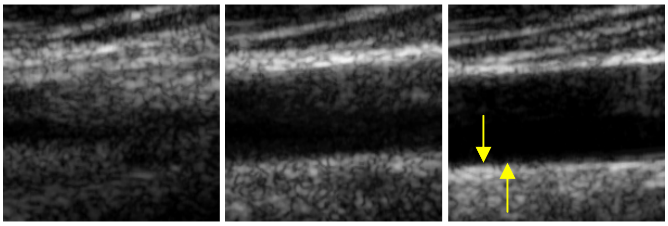

(a) (b) (c)

Figure 1. The ROI (200×200) cut from 3 of the 16 input frames. (a) and (b) show 2 outlier images; (c) an appropriate image with a mark of intima-media layer

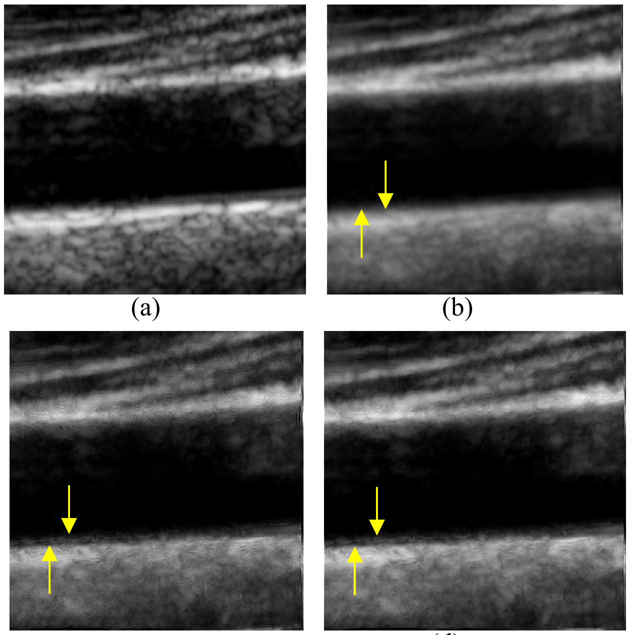

(a) (b) (c) (d)

Figure 2. The results (800×800) achieved by different algorithms with the same input and number of iteratation. (a) the interpolated image; (b) the fast SR algorithm proposed without robustness, adding the anisotropic diffusion regularzation; (c) the proposed algorithm without anisotropic diffusion (d) the fast and robust algorithm with anisotropic diffusion

B. *Results*

Fig. 2(a) shows the initial 800×800 image from the bicubic interpolation which shows less information about intima-media layer, especially on the left part. Fig. 2 (b) is from the original fast SR algorithm where the intima-media layer has been smoothed out due to the effect of including outlier images. Using our robust algorithm to deal with the outlier images, we can obtain much clearer interface between intimal and adventitial layer, see Figs. 2(c) and 2(d). The effect of using anisotropic diffusion regularization on Figs. 2(c) and 2(d) is not significant visually but the contrast close to intimal and adventitial layers in Fig. 2(d) is better than that in Fig. 2(c).

To further investigate anisotropic diffusion regularization used in our algorithm, we have conducted computer simulation of B-mode images of a common carotid artery with motion similar to real carotid. One of generated 16 images is shown in Fig. 3(a) with a small size of 200×50 and a reconstructed image with the size of 800×200, Fig. 3(b) for further analysis.

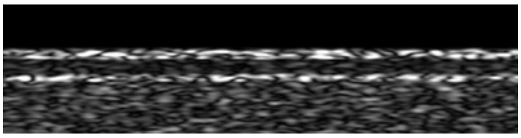

(a)

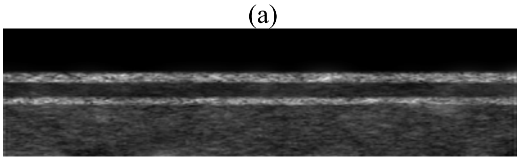

(b)

Figure 3. Intima-media layers in simulated carotid: (a) one of original image(200×50) and (b) reconstructed image from 16 frames (800×200) .

The effect of anisotropic diffusion regularization can be demonstrated by a comparison of the speckle statistics, Table I, which shows a lower contrast-to-noise (CNR) and higher standard deviation for SR without diffusion compared our algorithm. The CNR is given as:

$$CNR = (S_i - S_o) / \left(\sigma_i^2 + \sigma_o^2\right)^{\frac{1}{2}} \tag{14}$$

where S_i and S_o are the mean values inside and outside the carotid wall region, and σ_i and σ_o are the standard deviations, respectively.

TABLE I. SPECKLE STATISTICS FOR EACH METHOD

	Method			
	Original	***Interpolated***	***SR without diffusion***	***Proposed SR***
Mean	43.4506	43.4508	43.6672	43.4468
Std.	50.3695	50.0060	40.6490	39.3948
CNR	0.7233	0.7262	0.8161	0.8718

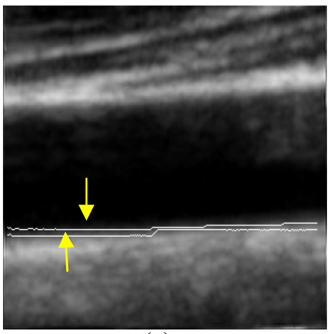

(a)

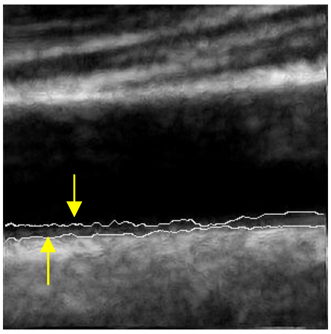

(b)

Figure 4. Boundary detection from (a) the original SR algorithm and (b) the robust SR algorithm.

The proposed algorithm can be used as a pre-processing step for boundary detection and IMT measurement. To demonstrate the robustness to outliers, a boundary detection algorithm of intima-media layer [10] was applied including outlier images, Figs. 1(a)(b) with results shown in Fig. 4. From Fig. 4(a), we see that the original SR algorithm is affected by the outliers and produces less accurate results. It is difficult to detect the accurate boundary and then measure its thickness. However, the boundary detection results from our robust SR algorithm can trace accurate intima-media layer, see Fig. 4(b).

IV. CONCLUSSION

SR algorithm is an effective approach to enhancing resolution used in medical images, but its accuracy is affected by speckle artifacts in ultrasound. We propose a fast method that does not require pre-selection and incorporate anisotropic diffusion during the reconstruction process to reduce the speckle while enhancing edges. It is valuable for measurement of IMT and early diagnoses of myocardial infarction or cardiovascular disease.

The robust method protects against outliers (some bad or inappropriate images) which is necessary in real clinical situations. Our future work is finding a fast and automatic approach to select images which have most similar shapes and most complementary information as a preprocessing step to reconstruction. Additionally, the boundary detection should also be improved.

REFERENCES

[1] M.Elad and A.Feuer, "Restoration of single super-resolution image from several blurred, noisy and down-sampled measured images," IEEE Trans. Imag. Proc., vol.6, no.12, pp. 1646-1658, Dec.1997.

[2] S.Farsiu, D.Robinson, M.Elad, and P.Milanfar, "Advances and challenges in superresolution", Int.J.Imag.Syst. Technol., vol.14, no.2, pp.47-57, Aug. 2004..

[3] Z.Yang, T.A.Tuthill, D.L.Raunig, M.D.Fox, and M.Analou, "Pixel compounding: Resolution-enhanced ultrasound imaging for quantitative analysis," Ultrason. In Med.&Biol.,vol.33,no.8, pp.1309-1319, Apr.2007.

[4] P.Vandewalle, S.Susstrunk, M. Vetterli. "A frequency domain approach to registration of aliased images with application to super-resolution," J. Appl. Signal Processing, vol.2006, pp.1-14, 2006.

[5] M.Elad, "A fast super-resolution reconstruction algorithm for pure translational motion and common space-Invariant Blur," IEEE Trans.Imag.Proc., vol. 10, no.8, pp.1187-1193, Aug. 2001.

[6] S. Farsiu, D. Robinson, M. Elad, P.Milanfar, "Fast and robust super-resoluiton," IEEE Trans. Imag. Proc., vol.13, no. 10, Oct.2004

[7] E.Aharoni, G.Abramorich, "Edge preserving super-resolution Image Reconstruction," Technical report, The vision research and image science laboratory, 1999

[8] A.Zomet, A.Rav-Acha, and S.Peleg, "Robust super-resolution", in Proceeding of the Int.Conf. on CVPR, vol.1, pp.645-650, Dec. 2001.

[9] P. Perona, J.Malik, "Scale-Space and Edge Detection Using Anisotropic Diffusion," IEEE Trans.Pattern Anal.Machine Interll.,vol.12, no.7, pp.629-639, Jul.1990.

[10] G. Liu, B. Wang, D.C. Liu, "Detection of Intima-Media Layer of Common Carotid Artery with Dynamic Programming Based Active Contour Model", CCPR, pp.1-6, Oct. 2008